*The 2020 World Congress on*
***Advances in Civil, Environmental, & Materials Research (ACEM20)***
*25-28, August, 2020, GECE, Seoul, Korea*

# Aero-elastic model design and wind tunnel test of a 1000 kV substation gantry

Liang-hao Zou[1)], *Feng Li [2)], Yin Chen[3)], Jie Song[4)] and Shu-guo Liang[5)]

[1), 2), 4, 5)] *School of Civil Engineering, Wuhan University, Wuhan, China*
[3)] *Central Southern China Electric Power Design Institute Co., LTD of China Power Engineering Consulting Group, Wuhan, China*
[2)] *lifeng8681@whu.edu.cn*

## ABSTRACT

This study aims to investigate wind-induced responses of a 1000 kV substation gantry via the aero-elastic model wind tunnel test. The advantages and disadvantages of the main methods in designing aero-elastic models were compared. An aero-elastic model that is able to simulate the first four-order frequency was designed and manufactured by the method of combining semi-rigid segments and V-shape springs. Based on this, structural displacement and acceleration responses of the typical segments in different wind speed and wind direction cases were investigated by the aero-elastic model wind tunnel test. Meanwhile, gust response factors were estimated both by the inertial wind load method and the gust loading factor method. Results show that the method of combining semi-rigid segments and V-shape springs satisfies the vital simulation parameters such as geometric shape, mass, frequency and damping ratio well. Wind direction plays an important role in the mean displacement, while the worst wind direction is at 15° to the corresponding axis. The root mean square of acceleration in the along-wind and cross-wind direction is in the same order of magnitude. In other words, the wind-induced vibration effect in cross-wind direction is obvious. In the direction perpendicular to the span, the central tower's wind-induced vibration mainly depends on the resonance component of the first mode. By contrast, the contributions of the basic order and higher modes are all significant for the side tower's wind-induced responses. The contribution of higher modes for the side tower's responses cannot be ignored. The range of the displacement gust response factor and the inertial force gust response factor is relatively close, which provides references for estimating the performance of similar substation gantries subjected to wind.

---

[1)] Associate Professor
[2)] Ph.D. Candidate
[3)] Ph.D.
[4)] Associate Professor
[5)] Professor

## 1 INTRODUCTION

Substation gantry is one of the essential structures for hanging conductors, supporting switchgears and other electrical equipment in a high voltage substation. To achieve these functions, the substation gantry is usually high, multi-span and spatially complex, and has the characteristic of both high-rise structures and large span structures, causing the high challenge in estimating accurate wind-induced responses of the substation gantry.

To date, the study of wind loads and wind-induced responses of the substation gantry is very limited (Kempner J. L., 2009). The wind-induced responses of the substation gantry are mainly investigated by applying simulated wind load on the finite element model (Niu et al, 2015; Pan et al, 2009). The wind load on the substation gantry is usually determined by means of the quasi steady theory based on the existing wind speed power spectral density (PSD). Although this method has economical efficiency, the cross-wind load has not been considered, which could cause considerable errors. By contrast, the aero-elastic model simulates both the structural dynamic and aero-elastic characteristics. The cross-wind loads on the structure can be inherently considered. Therefore, the aero-elastic model wind tunnel test is an effective and reliable method to evaluate the behaviors of the substation gantry subjected to the strong wind.

Substation gantry, especially for the power grid of ultra high voltage (UHV), is usually composed of several lattice towers and lattice crossbeams. The structure has small damping ratios and many connecting rods with various sizes, causing the difficulty in designing and manufacturing the aero-elastic model. Since the aero-elastic model of the substation gantry has been rarely manufactured before, this study adopts the methods for making an aero-elastic model of the lattice tower because of their similarity in basic lattice segments. There are three potential methods for designing the aero-elastic model: concentrated stiffness method (Lin et al, 2012; Wang et al, 2005), discrete stiffness method (Ahmad et al, 1984; Deng et al, 2010; Deng et al, 2016; Elawady et al, 2017; Huang et al, 2012; Liang et al, 2015; Lou et al, 1996; Xie et al, 2017) and the method of combining semi-rigid segments and V-shape springs (Li et al, 2011; Liang and Li, 2009).

Concentrated stiffness method uses only one variable cross-section rigid stick to simulate the whole structural stiffness and adds light plastic plates on the surface to simulate the whole shape, mainly used for single-rod towers with small change in the shape along the structural height, such as single-rod transmission towers (Lin et al, 2012; Wang et al, 2005). Although this method is relatively simple, the structural mode shapes of the model may be quite different from the actual mode shapes and the additional stiffness of the plastic plates can lead to the distortion of the aerodynamic forces on the central rigid stick. Discrete stiffness method aims to simulate the structural characteristics of all rods (Deng et al, 2010; Deng et al, 2016; Elawady et al, 2017; Huang et al, 2012; Liang et al, 2015; Lou et al, 1996; Xie et al, 2017). In other words, the stiffness, mass and geometric shape of every rod must be simulated by

assembling the hollow steel tubes, counter-weight lead wires and light plastic plates together. The aero-elastic model can simulate the structural modal properties accurately and hence the wind-induced structural failure experiment can be conducted on this model. Due to restriction of material characteristics, however, actual hollow steel tubes that meet geometric similarity is not rigid enough to meet stiffness similarity because of the stiffness loss in the assembling process. Meanwhile, too many rods and additional plastic plates may cause excessive structural damping ratios that cannot meet the requirements for damping ratios of steel structures. Thus, discrete stiffness method is appropriate for making an aero-elastic model of single lattice towers. For the substation gantry with multi spans, excessive damping ratios may appear in the model by this method, due to the large number of stressed rods and many energy consuming parts. Another method is combining semi-rigid segments and V-shape springs. The whole structure is divided into several semi-rigid segments based on the geometric similarity, and the mass distribution is consistent with the prototype. The segments are connected with V-shaped springs that provide the stiffness of the model (Li et al, 2011; Liang and Li, 2009). The whole aero-elastic model is similar to a simplified multi-particle model, which does not simulate the stiffness distribution of every rod accurately. The aero-elastic model, however, has the advantages of simple connection between segments and hence less energy consumption. When the stiffness of the model is determined by several specific V-shape springs, the model can simulate the structural modal properties well. For the substation gantry with multi spans, the aero-elastic model by this method avoids insufficient stiffness of the material and excessive damping ratios by discrete stiffness method, and reflects wind-induced response characteristics of the whole structure well. Based on the above analysis, the method of combining semi-rigid segments and V-shape springs is an appropriate choice for the aero-elastic model of the substation gantry.

In this study, an aero-elastic model of a 1000 kV substation gantry is designed and manufactured by the method of combining semi-rigid segments and V-shape springs. The displacement and acceleration responses in the typical structural locations in different wind speed and wind direction cases are investigated by the aero-elastic model wind tunnel test. Meanwhile, the gust response factors are estimated both by the inertial wind load method and the gust loading factor method. The results provide references for estimating the performance of similar substation gantries subjected to wind.

## 2 WIND TUNNEL TESTS

### *2.1 Design and manufacture of the aero-elastic model*

The 1000 kV substation gantry in this study is a 61 m high lattice frame structure made of thin-walled steel tubes as shown in Fig. 1. The gantry has two spans and each span is 51 m. According to the similarity theory, the aero-elastic model should satisfy not only the basic geometric, stiffness and mass similarity conditions, but also the demands of Strouhal number, Cauchy number, Froude number, Reynolds number and the damping ratio. And the key parameters should be ensured to simulate accurately as

the requirements of all the parameters cannot be satisfied concurrently. In this study, the similarities of Strouhal number, Cauchy number, Froude number and the damping ratio are all simulated strictly. Due to the restriction of the wind tunnel, it is difficult to use high wind speed to meet the Reynolds number similarity directly, although the Reynolds number effects should not be ignored on the substation gantry made of steel tubes. Since the value of aerodynamic force coefficients is closely related to the Reynolds number effects, the experimental results are modified by equivalent aerodynamic force coefficients to consider the Reynolds number effects based on the existing studies (Huang et al, 2012; Simiu and Scanlan, 1978; Sykes, 1981). The geometric similarity ratio is 1/50, considering the height and width of the prototype substation gantry and the restricted size of the wind tunnel. The main similarity ratios are listed in Table 1.

Fig. 1 Prototype of the 1000 kV substation gantry

Table 1 Similarity ratios of key parameters of the aero-elastic model

| Parameter | Scale ratio | Parameter | Scale ratio |
|---|---|---|---|
| Length | $\lambda_L = L_m/L_p = 1/50$ | Frequency | $\lambda_f = f_m/f_p = 6.99$ |
| Area | $\lambda_A = L_m^2/L_p^2 = 1/2500$ | Velocity | $\lambda_v = \lambda_f\lambda_L = 1/7.15$ |
| Air density | $\lambda_\rho = \rho_m/\rho_p = 1$ | Elastic Stiffness | $\lambda_{EA} = \lambda_v^2\lambda_L^2 = 1/127806$ |
| Structural density | $\lambda_{\rho s} = \rho_{ms}/\rho_{ps} = 1.17$ | Displacement | $\lambda_y = \lambda_v/\lambda_f = 1/50$ |
| Mass | $\lambda_M = \lambda_{\rho s}\lambda_L^3 = 1.17/125000$ | Acceleration | $\lambda_a = \lambda_f^2\lambda_L = 0.98$ |

Subscripts m, and p represent the model and the prototype scale, respectively.

After the similarity ratios have been determined, geometric shape, stiffness, mass and damping ratio of the aero-elastic model should be seriously followed in manufacturing the model.

In the geometric shape simulation, prototype rods are classified in the diameter, and hence the diameter of the model rods can be determined by the geometric similarity ratio. The diameters of some rods are so close that the difference of these rods can be ignored in the 1/50 geometric similarity ratio. In other words, the types of rods can be

simplified. According to the structural characteristics of the substation gantry, the whole structure in this study is divided into 21 typical semi-rigid segments. Each semi-rigid segment consists of thin-walled stainless steel tubes as rods by lead-free solder for connection.

The model stiffness is provided by specific V-shape springs between semi-rigid segments. The V-shape springs should meet the requirements of bending and axial stiffness similarity ratios. In detail, a finite element model of the prototype substation gantry is firstly established by a finite element software, as shown in Fig. 2(a). The structural modal properties of the prototype model can be analyzed, and hence the structural modal properties of the aero-elastic model can be obtained based on the similarity ratio. Then, a finite element model of the aero-elastic model with V-shape springs can be established to meet the requirement of the similarity ratio by adjusting the basic parameters of V-shape springs, such as thickness, width and V-bend angle, as shown in Fig. 2(b). Owning to the stiffness loss in assembling V-shape springs to the semi-rigid segments, 10% of the excessive stiffness is considered in designing. Finally, three kinds of specific V-shaped springs are determined as can be seen in Fig. 3. In total, 136 V-shape springs made of spring steel are used, including 32 No. 1 springs, 56 No. 2 springs and 48 No. 3 springs. Although the springs increase additional windward area on the aero-elastic model, the windward area of all springs together is controlled under 2% as that of the whole aero-elastic model no matter in the along-wind direction or in the cross-wind direction, indicating that the springs cannot cause too many additional aerodynamic forces on the aero-elastic model and hence the influence of additional windward area by springs can be ignored.

In the mass similarity simulation, the mass distribution of the aero-elastic model should be consistent with the prototype and each segments should meet the requirements of the mass similarity ratio. The mass of V-shaped springs also has been considered in the design stage before fabricating the model. In the manufacture process, some segment models are slightly heavier than the expected ones, but the total mass is relatively close, which is acceptable.

Generally, the damping ratio of the aero-elastic model cannot be controlled at the design stage except for the known material properties. It should be noticed to reinforce the connection between semi-rigid segments and V-shaped springs as possible in the manufacture process to reduce the friction in the connection parts. The method of combining semi-rigid segments and V-shape springs has the advantages of simple connection between segments and less energy consumption, so this method can achieve a good effect in simulating structures with low damping ratios such as the substation gantry.

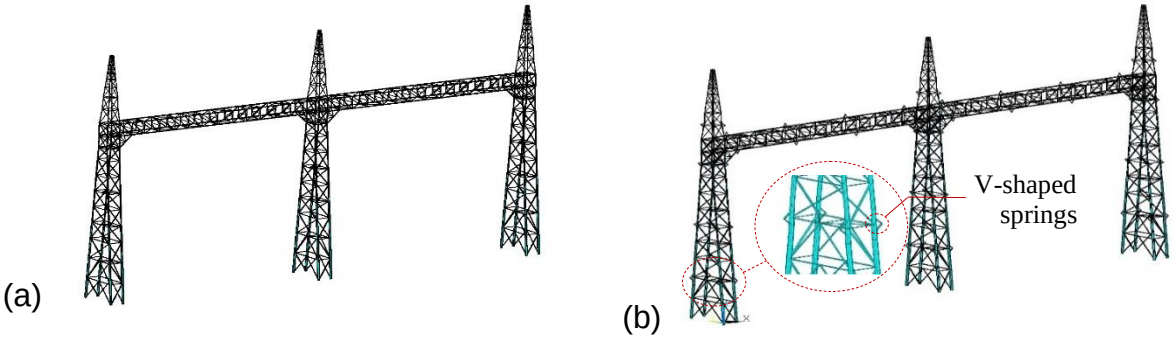


Fig. 2: (a) The prototype finite element model; (b) The finite element model of the aero-elastic model

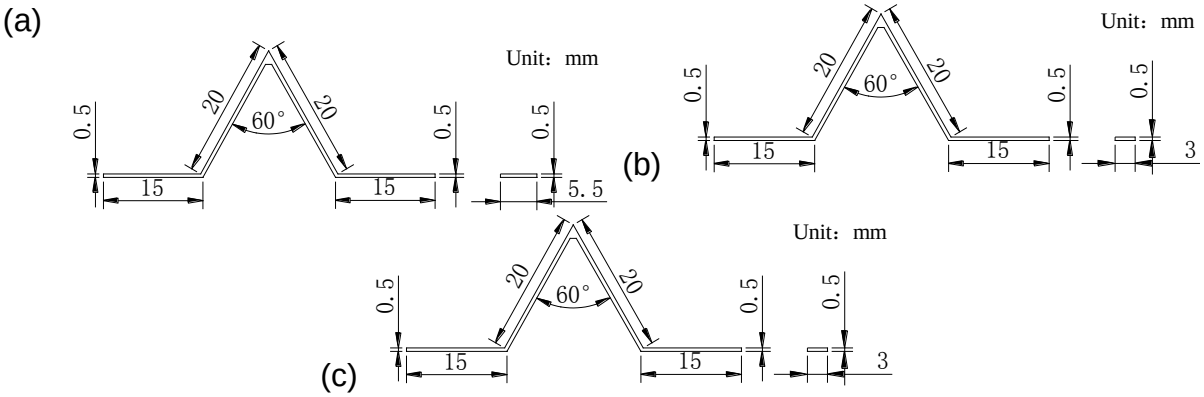


Fig. 3 Three kinds of specific V-shaped springs named: (a) No. 1; (b) No. 2; (c) No. 3.

After fabricating the aero-elastic model, the impact hammer tests are conducted to identify structural modal properties. The first four-order frequency and the first two-order damping ratio of the aero-elastic model are determined through parameter identification, as listed in Table 2. The main modal frequency of the aero-elastic model is close to the theoretical value, and the relative error is within 3%. Meanwhile, the value of structural damping ratio is smaller than 1%, which is acceptable. The first four-order mode shape is shown in Fig. 4. Finally, an aero-elastic model of the substation gantry is completed as shown in Fig. 5.

Table 2 The natural frequency and the damping ratio

| Mode | 1st | 2nd | 3rd | 4th |
|---|---|---|---|---|
| Prototype/Hz | 1.13 | 1.54 | 1.73 | 2.18 |
| Mode/Hz | 7.70 | 10.74 | 12.45 | 15.38 |
| Relative errors/% | -2.58 | -0.23 | 2.87 | 0.92 |
| Damping ratios/% | 0.85 | 0.88 | — | — |

Relative errors = $(f_m - f_p\lambda_f)/f_m$

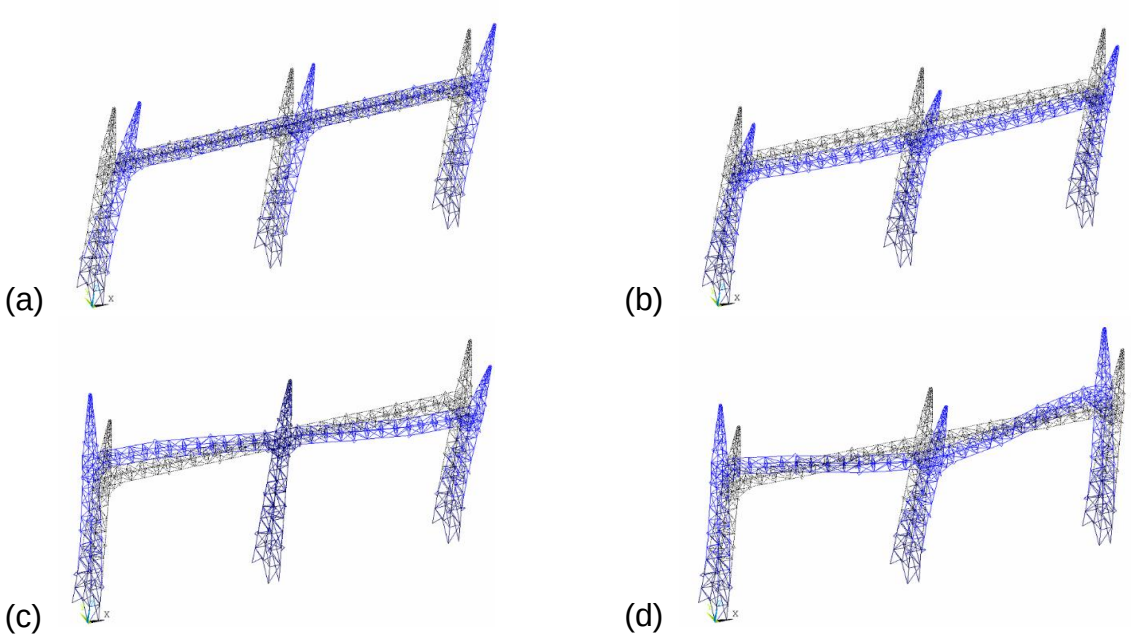

Fig. 4 The first four-order mode shape of the substation gantry: (a) 1st mode; (b) 2nd mode; (c) 3rd mode; (d) 4th mode.

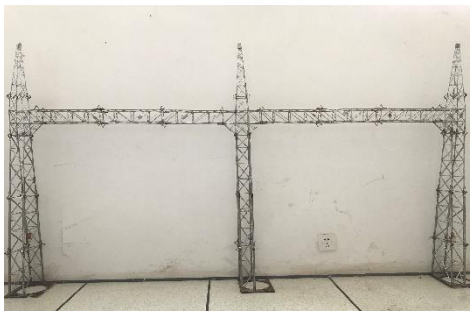

Fig. 5 Aero-elastic model of the substation gantry

*2.2 Aero-elastic model wind tunnel test*

The aero-elastic model wind tunnel test is conducted in the WD-1 wind tunnel in Wuhan University. The wind tunnel has a test-section of 16 m long with a cross-section of 3.2 m wide ×2.1 m high, in which the wind speed can be continuously adjusted in the range of 1 m/s to 30 m/s. In the wind tunnel, a plurality of sharp tower vortex generators and distributed cubic roughness elements are adopted to simulate the atmospheric boundary layer wind field. Since the substation gantry is located in a flat area, Category B of terrain (exponent α= 0.15) is considered in the test, according to China's code (GB50009, 2012). The mean wind speed and turbulence intensity of the oncoming flow is shown in Fig. 6(a), and the PSD of wind speed is shown in Fig. 6(b).

The aero-elastic model wind tunnel test, shown in Fig. 7, is carried out in the wind directions of -90° to 90° at 15° increments. The definition of the wind direction and structural coordinate are shown in Fig. 8. Five levels of wind speed are considered, i.e., 3 m/s, 4 m/s, 5 m/s, 6 m/s and 8 m/s. The displacements and accelerations in six typical measuring points of the model are all tested, as illustrated in Fig. 9. Specifically,

Y1 and Y2 are the top measuring points of the central tower and side tower in the Y-axis; Y3 and Y4 are the measuring points of the joints with crossbeams of the central tower and side tower in the Y-axis; X1 is the top measuring point of the side tower in the X-axis; X2 is the measuring point of the joint with crossbeams of the side tower in the X-axis. The height of the cobra probe device is determined at 1.22 m, the same height at the top of the aero-elastic model. The sampling frequency of the laser displacement sensors is 500 Hz, whereas that of the acceleration sensors is 512 Hz. The duration of all response measurement is 90 s.

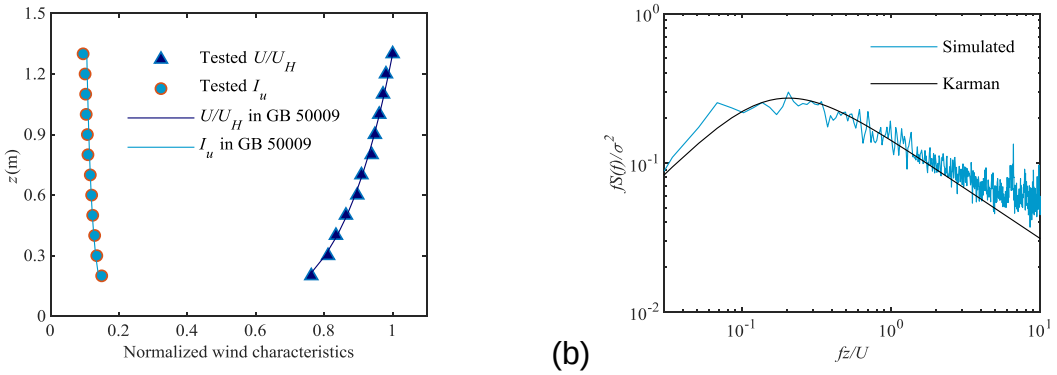


(a) (b)

Fig. 6: (a) The profile of mean wind speed and turbulence intensity; (b) PSD of wind speed

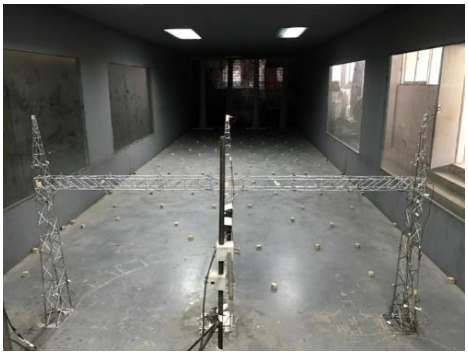

Fig. 7 The aero-elastic model wind tunnel test

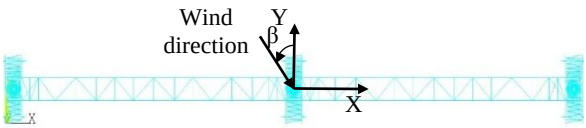


Fig. 8 Definition of the wind direction and structural coordinate

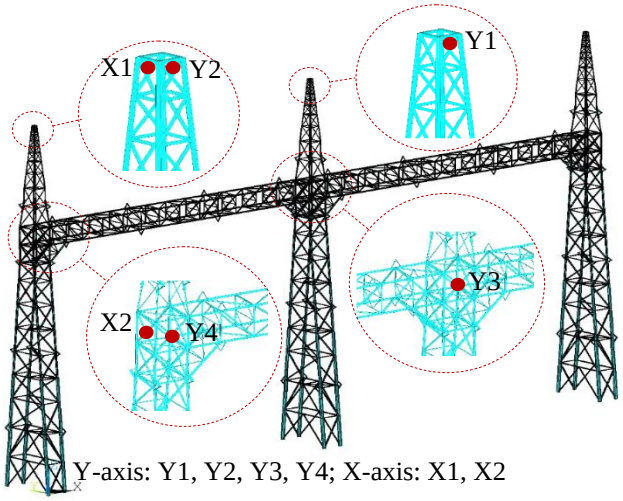


Fig. 9 Arrangement of the measuring points

## 3 RESULTS OF AERO-ELASTIC TEST

After measuring displacement and acceleration response time series of the aero-elastic model in the wind tunnel test in various cases, the mean displacements, RMS accelerations of the 1000 kV substation gantry under wind actions can be obtained by data processing.

### *3.1 Displacement response*

The mean displacements of all measuring points in the wind directions of -90°, 0° and 90° as the wind speed increases are shown in Fig. 10. Clearly, the mean displacements in the along-wind direction are growing as the wind speed increases, whereas the mean displacements in the cross-wind direction are still close to 0 and independent with the wind speed. In addition, the mean displacements of the central tower (Y1 and Y3) are greater than that of the side tower (Y2 and Y4) at the same height in 0° wind direction.

The mean displacements of top measuring points (Y1, Y2 and X1) in the wind directions of -90° to 90° at 15° increments are shown in Fig. 11. In general, the mean displacement value of the substation is sensitive to the wind direction. For the measuring points of central tower (Y1) and side tower (Y2) in the Y-axis, the change law of mean displacements with the wind direction is basically the same: In the wind directions of -90° to 0°, the mean displacements are increasing and reach the maximum at -15°; in the wind directions of 0° to 90°, the change law of that is nearly symmetrical with the wind direction of -90° to 0°. In the X-axis, the change law of mean displacements is also symmetrical, reaching the maximum at -75° or 75°. That is mainly because the frontal windward area of the substation gantry reaches the maximum at -15° or 15°, while the lateral windward area reaches the maximum at -75° or 75°.

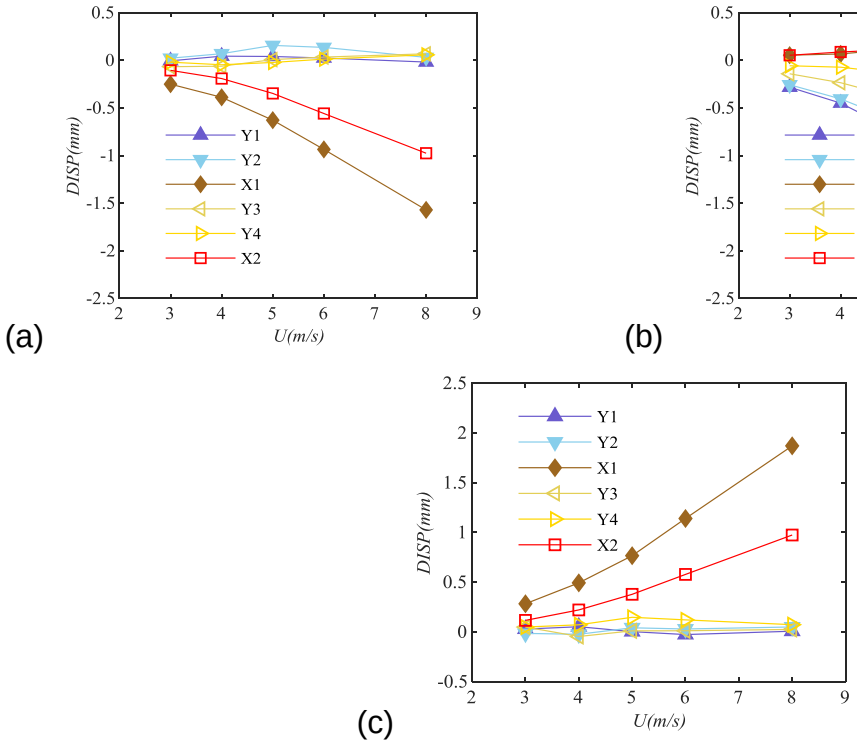


Fig. 10 Mean displacement response in typical wind direction: (a) -90°; (b) 0°; (c) 90°.

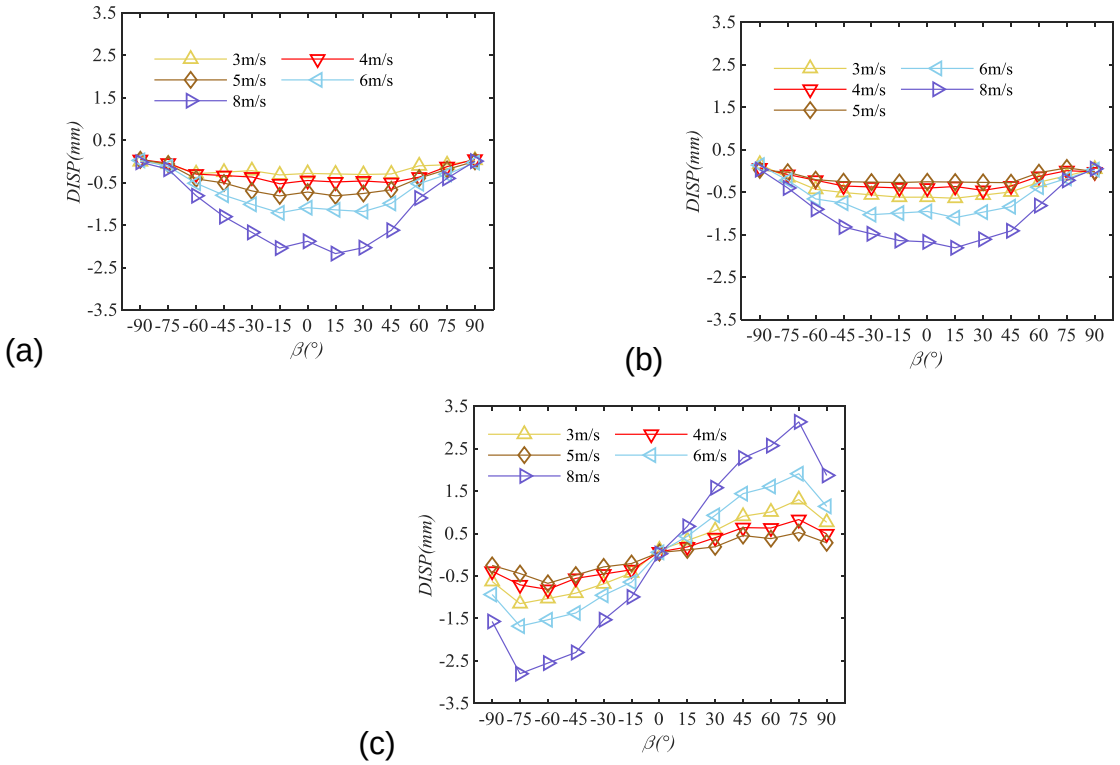


Fig. 11 Mean displacement response of top measuring points: (a) Y1; (b) Y2; (c) X1.

*3.2 Acceleration response*

The root mean square (RMS) of acceleration response of all measuring points in the wind directions of -90°, 0° and 90° as the wind speed increases is shown in Fig. 12. Obviously, the RMS of acceleration response is growing as the wind speed increases. The RMS value of the central tower (Y1 or Y3) is close to that of the side tower (Y2 or Y4) at the same height. The RMS value of the joints between towers and crossbeams is about 40% to 60% of that of the top measuring points in the one tower.

The root mean square (RMS) of acceleration response of top measuring points (Y1, Y2 and X1) in the wind directions of -90° to 90° at 15° increments are shown in Fig. 13. The RMS value increases slightly in the wind directions of -90° to 0°, and in the wind direction ofs 0° to 90°, the change law of the RMS value is nearly symmetrical with the wind direction of -90° to 0°.

Furthermore, as can be seen in Figs. 12 and 13, the RMS acceleration responses in the along-wind direction and cross-wind direction at 0° are in the same order of magnitude, indicating that the cross-wind vibration effect of the substation gantry cannot be ignored. The main reasons are as follows: The first order frequency is 1.54 Hz in the along-wind direction, where as that is 1.13 Hz in the cross-wind direction. In other words, the cross-wind stiffness is greater than the along-wind stiffness. Meanwhile, the substation gantry is composed of three towers and two crossbeams. The cross section of each tower is rectangular (the long side is in the cross-wind direction), so the windward area in the cross-wind direction of each tower is larger than that in the along-wind direction. Although the windward area of crossbeams in the along-wind direction is significant, the total windward area in the cross-wind direction is not much smaller than that in the along-wind direction.

To study the characteristics of the wind-induced responses in the frequency domain further, spectral analysis of the acceleration response at the top of the aero-elastic model is carried out. The acceleration response PSDs of top measuring points (Y1, Y2 and X1) at 0° at the wind speed of 6 m/s (42.9 m/s at the top of the structure for actual wind field) are shown in Fig. 14. In the Y-axis, the acceleration response at the top of the central tower (Y1) is mainly contributed by the resonance component of the first mode in this direction, and the contribution of the higher-order mode is small; The acceleration response at the top of the side tower (Y2) is contributed by the resonance component of the first three modes in this direction, and the contribution of the higher-order mode cannot be ignored. In the X-axis, the acceleration response at the top of the side tower is contributed by the resonance component of the first mode in this direction.

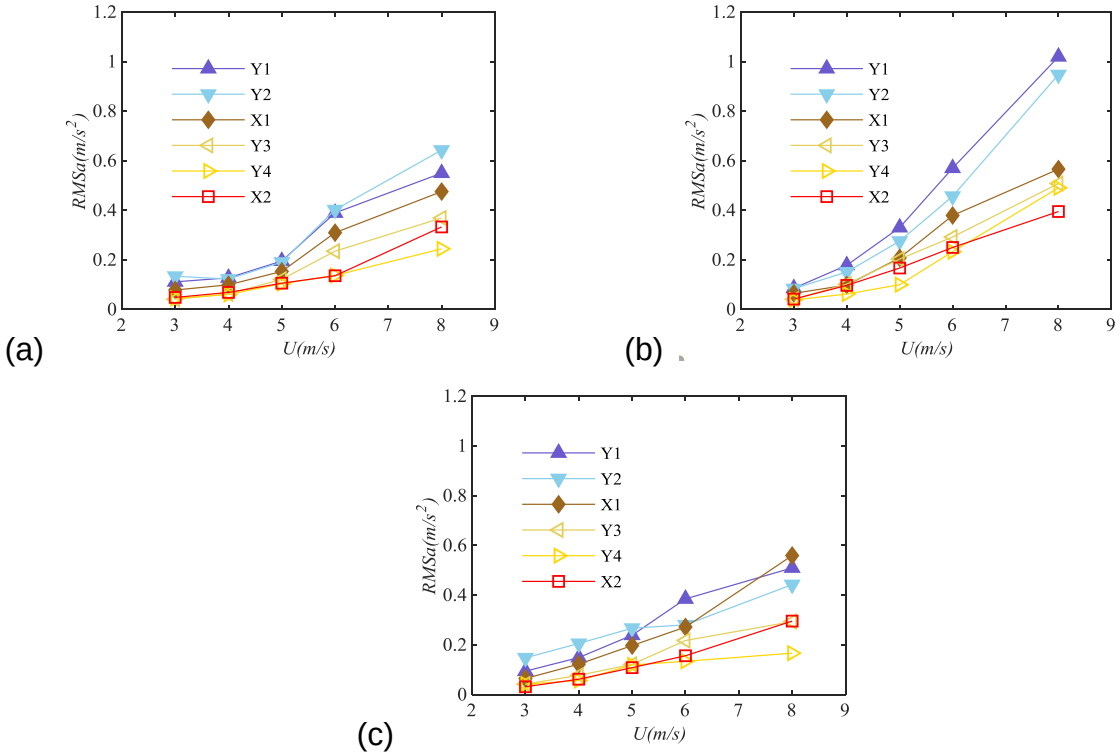


Fig. 12 Acceleration root mean square in typical wind direction: (a) -90°; (b) 0°; (c) 90°.

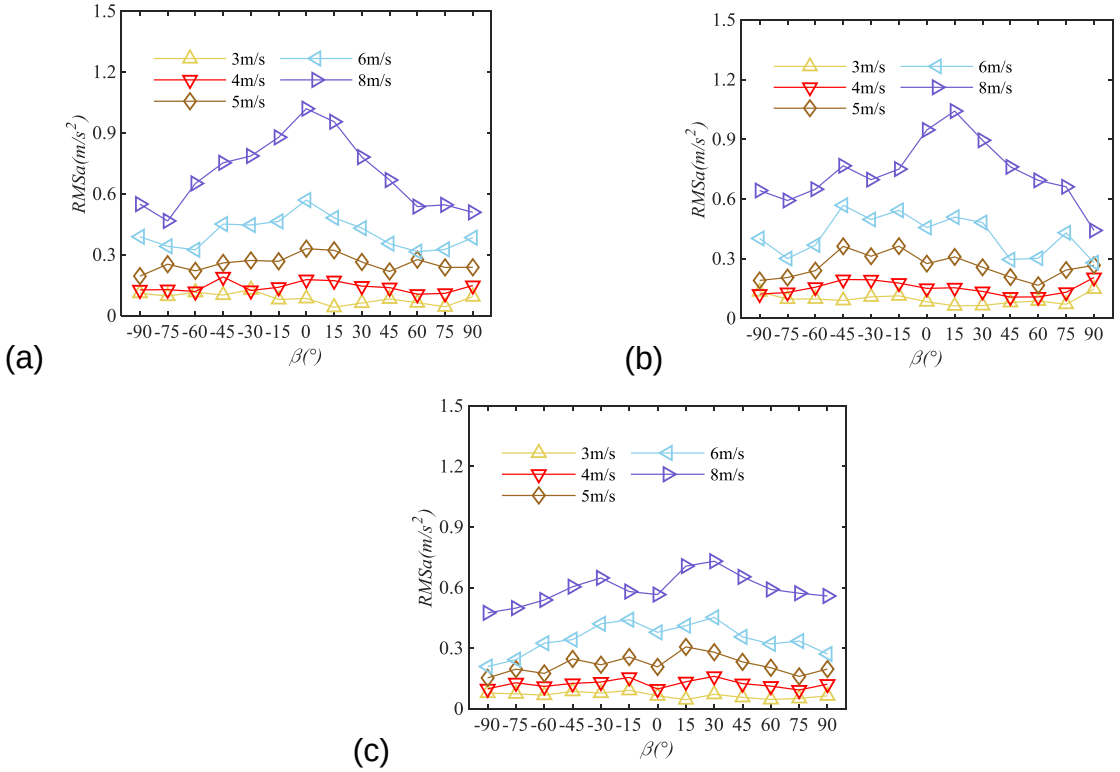


Fig. 13 Acceleration root mean square of top measuring points: (a) Y1; (b) Y2; (c) X1.

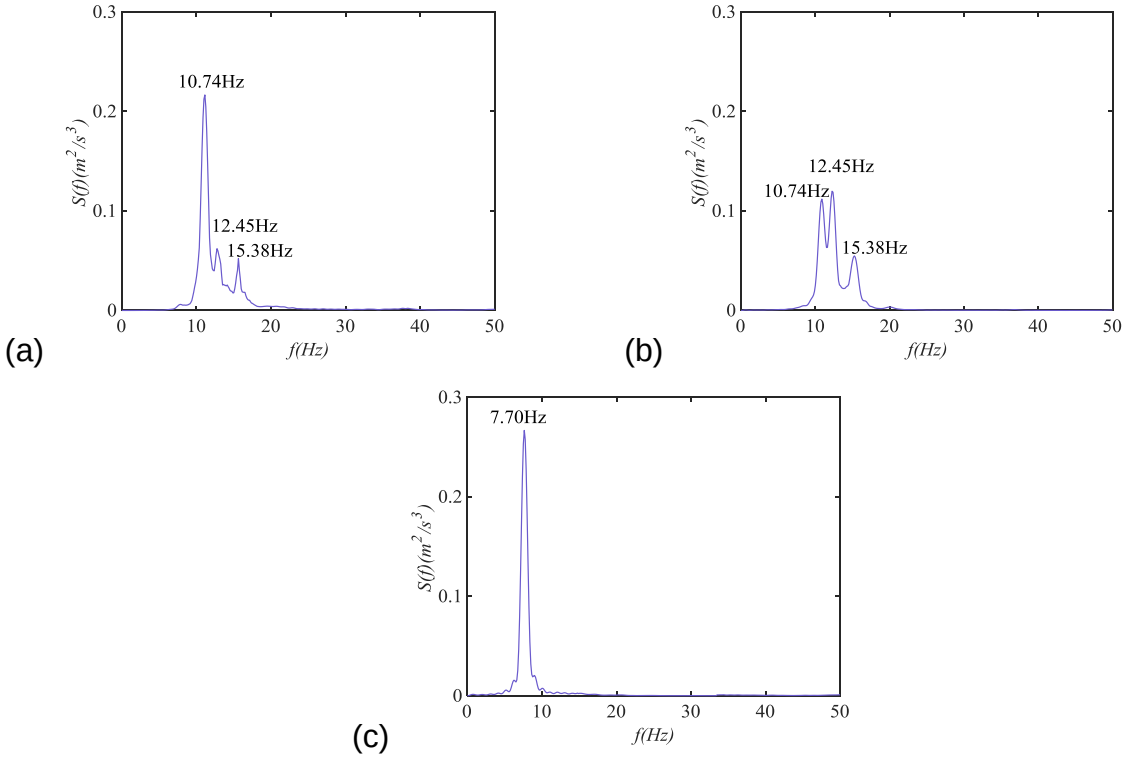


Fig. 14 Acceleration PSD of top measuring points: (a) Y1; (b) Y2; (c) X1.

*3.3 Gust response factor*

The gust response factor (Davenport, 1967; GB50009, 2012; Vellozzi and Cohen, 1968) aims to simplify the fluctuating wind load into the static load effect based on some principles, playing an important role in engineering designs. To date, the gust response factor of the substation gantry is not clear, compared with that of the free standing single tower. Thus, the gust response factor of the substation gantry is often determined by engineering experience. The gust response factor in this study is estimated directly based on the measured wind-induced responses by the aero-elastic model wind tunnel test, providing references for design. Both the inertial wind load method in Eq. 1 and the gust loading factor method in Eq. 2 are used to estimate the gust response factor as listed in Table 3.

$$\beta_L(z) = 1 + g\frac{M(z)\sigma_a(z)}{\mu_s(z)\mu_z(z)w_0A(z)} \tag{1}$$

Where $\beta_L(z)$ is the gust response factor based on the inertial wind load method; $g$ is the peak factor and equals 3.5 in this study; $M(z)$ is the concentrated mass at the structural height $z$; $\sigma_a(z)$ is the RMS of the acceleration response in the along-wind direction; $\mu_s(z)$ is the shape coefficient at $z$, determined by the study (Chen and Zhu,

2019); $\mu_z(z)$ is the exposure factor for wind pressure at $z$; $w_0$ is the basic wind pressure; $A(z)$ is the windward area of the rods at $z$.

$$\beta_D(z) = 1 + g\frac{\sigma_y}{|\bar{y}|} \tag{2}$$

Where $\beta_D(z)$ is the gust response factor based on the gust loading factor method; $\sigma_y$ is the RMS of the displacement response; $\bar{y}$ is the mean displacement response.

As can be seen in Table 3, the range of $\beta_L(z)$ is 1.35 to 1.58, whereas that of $\beta_D(z)$ is 1.40 to 1.59, showing that the range of the results based on the two methods is relatively close. But in detail, the value of $\beta_L(z)$ is slightly smaller than that of $\beta_D(z)$ for the same segment in the same wind direction, mainly because $\beta_L(z)$ includes the contribution of the resonance component only, while the contribution of both the resonance component and the background component is considered in $\beta_D(z)$.

Table 3 Gust response factor

| Wind direction | Measuring points | $\beta_L(z)$ | $B_D(z)$ |
|---|---|---|---|
| 0° | Y1 | 1.46 | 1.53 |
| | Y2 | 1.46 | 1.40 |
| | Y3 | 1.42 | 1.46 |
| | Y4 | 1.35 | 1.51 |
| -90° | X1 | 1.42 | 1.57 |
| | X2 | 1.58 | 1.59 |
| 90° | X1 | 1.43 | 1.49 |
| | X2 | 1.50 | 1.54 |

## 4 CONCLUSIONS

An aero-elastic model of a typical 1000 kV substation gantry is designed and manufactured by the method of combining semi-rigid segments and V-shape springs. The wind-induced responses and the gust response factors of the substation gantry are investigated by the the aero-elastic model wind tunnel test. The main conclusions are as follows:

The first four-order frequency of the designed and manufactured aero-elastic model in the study meets the theoretical analysis result well. The method of combining semi-rigid segments and V-shape springs not only avoids the problems of insufficient stiffness and excessive damping ratio of the material, but also ensures high accuracy in reflecting wind-induced response characteristics of substation gantries, indicating the high suitability in producing aero-elastic models of similar structures.

Wind direction plays an important role in the mean value of displacement, and the worst wind direction of the mean displacement is 15° to the corresponding principal

axis. For the acceleration responses, however, the RMS acceleration changes slightly in the wind directions of -90° to 90°. In the wind direction of 0°, the along-wind RMS acceleration of the central tower (Y1 or Y3) is close to that of the side tower (Y2 or Y4) at the same height. Meanwhile, the along-wind and cross-wind RMS acceleration responses at 0° are in the same order of magnitude. In other words, the effect of cross-wind vibration is significant, which should be noticed further in the design. What's more, for the substation gantry composed of three towers and two crossbeams, the central tower's wind-induced vibration is dominated by the resonance component of the first mode in direction of perpendicular to the span, whereas the contribution of high-order modes cannot be ignored for the side towers' vibration in this direction. In addition, the gust response factors by the the inertial wind load method and the gust loading factor method: $\beta_L(z)$ and $\beta_D(z)$, are both between 1.35 to 1.59, providing references for estimating the performance of similar substation gantries subjected to wind.

## REFERENCES

Kempner J. L. (2008), Substation structure design guide. ASCE, Reston, Virginia.
Ahmad, M.B., Pande, P.K., Krishna, P. (1984). Self-Supporting Towers Under Wind Loads. Journal of Structural Engineering, **110**(2), 370-384.
Chen, Y., Zhu, D. (2019), Research on shape-coefficient of 1000 kV substation steel pipe frame by wind tunnel tests. Special Structures, **36**(2), 69-74. (In Chinese)
Davenport, A.G. (1967), Gust loading factors. Journal of the Structural Division, **93**(3), 11-34.
Deng, H., Si, R., HU, X., Chen, Q. (2010), Wind tunnel test on aeroelastic model of UHV latticed transmission tower. Journal of Tongji University (Natural Science), **38**(5), 673-678. (In Chinese)
Deng, H.Z., Xu, H.J., Duan, C.Y., Jin, X.H., Wang, Z.H. (2016), Experimental and numerical study on the responses of a transmission tower to skew incident winds. Journal of Wind Engineering & Industrial Aerodynamics, **157**, 171-188.
Elawady, A., Aboshosha, H., El Damatty, A., Bitsuamlak, G., Hangan, H., Elatar, A. (2017), Aero-elastic testing of multi-spanned transmission line subjected to downbursts. Journal of Wind Engineering and Industrial Aerodynamics, **169**, 194-216.
GB50009, (2012), Load code for the design of building structures. China Architecture & Building Press, Beijing, China. (In Chinese)
Huang, M.F., WenjuanLou, LunYang, BingnanSun, GuohuiShen, Tse, K.T. (2012), Experimental and computational simulation for wind effects on the Zhoushan transmission towers. Structure & Infrastructure Engineering, **8**(8), 781-799.
Li, Z., Ren, K., Xiao, Z., Wang, Z., Yu, K. (2011), Aeroelastic model design and wind tunnel tests of UHV transmission line system. Acta Aerodynamica Sinica, **29**(1), 102-106+113. (In Chinese)
Liang, S., Zou, L., Wang, D., Cao, H. (2015), Investigation on wind tunnel tests of a full aeroelastic model of electrical transmission tower-line system. Engineering Structures, **85**, 63-72.
Liang, Z., Li, Z. (2009), An aeroelastic model design of ultra-high voltage power tranmission line systems. Journal of Chongqing University, **32**(2), 131-136. (In Chinese)

Lin, W.E., Savory, E., Mcintyre, R.P., Vandelaar, C.S., King, J.P.C. (2012), The response of an overhead electrical power transmission line to two types of wind forcing. Journal of Wind Engineering & Industrial Aerodynamics, **100**, 58-69.
Lou, W., Sun, B., Tang, J.C. (1996), Wind tunnel test and numerical computation on wind-induced vibration for tall lattice tower. Journal of Vibration Engineering, **9**(3), 318-322. (In Chinese)
Niu, H., kong, K., Chen, Y., Chen, Z. (2015), 500 kV whole combined substation framework shape factor of wind tunnel test and dynamic response factor analysis. Journal of Hunan University (Natural Sciences), **42**(11), 80-87. (In Chinese)
Pan, F., Tong, J., Sheng, X., Ye, Y., Sun, B., Chen, Y. (2009), Wind-induced dynamic response of large thin-walled steel tube frame for 1000kV substation. Engineering Mechanics, **26**(10), 203-210. (In Chinese)
Simiu, E., Scanlan, R.H. (1978), Wind effects on structures: an introduction to wind engineering. Proceedings of the Institution of Mechanical Engineers, **185**(92), 301-317.
Sykes, D.M. (1981), Lattice frames in turbulent airflow. Journal of Wind Engineering & Industrial Aerodynamics, **7**, 203-214.
Vellozzi, J., Cohen, E. (1968), Gust response factors. Journal of the Structures Division, ASCE, 1295-1313.
Wang, S., Sun, B., Lou, W., Ye, Y. (2005), Wind tunnel test and theoretical analysis on aeroelastic model of single-rod transmission tower. Journal of Zhejiang University (Engineering Science), **39**(1), 88-92. (In Chinese)
Xie, Q., Cai, Y., Xue, S. (2017), Wind-induced vibration of UHV transmission tower line system: Wind tunnel test on aero-elastic model. Journal of Wind Engineering & Industrial Aerodynamics, **171**, 219-229.